


RESEARCH PAPER

Ursolic acid promotes apoptosis and mediates transcriptional suppression of CT45A2 gene expression in non-small-cell lung carcinoma harbouring EGFR T790M mutations

Kaiyong Yang¹ | Yan Chen² | Jiaqian Zhou¹ | Lin Ma¹ | Yating Shan¹ | Xiaoying Cheng¹ | Yun Wang¹ | Zhaoxin Zhang¹ | Xiaojun Ji¹ | Lili Chen¹ | Hui Dai¹ | Biqing Zhu¹ | Chen Li¹ | Zhonghua Tao^{3,4} | Xichun Hu^{3,4} | Wu Yin¹ 

¹State Key Lab of Pharmaceutical Biotechnology, College of Life Sciences, Nanjing University, Nanjing, China

²Division of nutrition, Jiangsu Cancer Hospital and Jiangsu Institute of Cancer Research and Nanjing Medical University Affiliated Cancer Hospital, Nanjing, China

³Department of Medical Oncology, Fudan University Shanghai Cancer Center, Shanghai, China

⁴Department of Oncology, Shanghai Medical College, Fudan University, Shanghai, China

Correspondence

Wu Yin, Lab of Biochemical and Molecular Pharmacology, State Key Lab of Pharmaceutical Biotechnology, College of Life Sciences, Nanjing University (Xianlin Campus), 168# Xianlin Ave, Room No. A310-1, Nanjing 210046, China.
Email: wyin@nju.edu.cn

Xichun Hu, Department of Medical Oncology, Fudan University Shanghai Cancer Center, 270 Dong'an Road, Shanghai 200032, China.
Email: xchu2009@hotmail.com

Funding information

Key Development Project of Jiangsu Province, Grant/Award Number: BE2017712; Six Talent Peaks Project in Jiangsu Province, Grant/Award Number: YY-012; Fundamental Research Funds for the Central Universities; National Natural Science Foundation of China, Grant/Award Numbers: 81403347, 81473293, 81573604, 81671939, 81673462, 81774269, 91540119, 81874452

Background and Purpose: In non-small-cell lung carcinoma (NSCLC) patients, the L858R/T790M mutation of the epithelial growth factor receptor (EGFR) is a major cause of acquired resistance to EGFR-TKIs treatment that limits their therapeutic efficacy. Identification of drugs that can preferentially kill the NSCLC harbouring L858R/T790M mutation is therefore critical. Here, we have evaluated the effects of ursolic acid, an active component isolated from herbal sources, on erlotinib-resistant H1975 cells that harbour the L858R/T790M mutation.

Experimental Approach: Gene expression omnibus (GEO) profiles analyses was applied to detect differentially expressed genes in NSCLC cells harbouring EGFR mutation. AnnexinV-FITC/PI, TUNEL staining, MTT, wound healing, RT-PCR, qRT-PCR, western blots, immunostaining, dual-luciferase reporters and ChIP-PCR were utilized to investigate the effects of ursolic acid in vitro and in vivo.

Key Results: The cancer/testis antigen family 45 member A2 (CT45A2) was highly expressed in H1975 cells. Ectopic expression of CT45A2 in H1975 cells increased cell proliferation and motility in vitro. Silencing the CT45A2 expression strongly attenuated H1975 cells motility and growth. The anti-cancer effect of ursolic acid was critically dependent on CT45A2 expression in H1975 cells. Ursolic acid suppressed CT45A2 gene transcription mediated by transcriptional factor TCF4 and β -catenin signalling.

Conclusions and Implications: CT45A2 is a novel oncogene for NSCLC with an EGFR T790 mutation. Ursolic acid induced apoptosis and inhibited proliferation of H1975 cells by negatively regulating the β -catenin/TCF4/CT45A2 signalling pathway. Therefore, ursolic acid may be a potential candidate treatment for NSCLC harbouring the EGFR-L858R/T790M mutation.

Abbreviations: AA, asiatic acid; AA, asiatic acid; CT45A2, cancer/testis antigen family 45 member A2; CTA, cancer/testis antigen; GSK, glycogen synthase kinase; MTT, 3-(4,5-dimethylthiazol-2-yl)-2,5-diphenyl tetrazolium bromide; NSCLC, non-small cell lung carcinoma; TAA, tumour-associated antigens; UA, ursolic acid; TKI, tyrosine kinase inhibitor; TUNEL, terminal deoxynucleotidyl transferase-mediated dUTP-biotin nick end labelling assay.

1 | INTRODUCTION

The widespread screening of patients with lung adenocarcinoma for the activation of mutations in **EGF receptors** (EGFR) has exposed those cancers driven by the T790M mutation as a growing clinical problem (Hata *et al.*, 2016; Pao *et al.*, 2005). Irreversible EGFR inhibitors are under active development to overcome the resistance to reversible tyrosine kinase inhibitors (TKIs) of EGFRs harbouring T790M mutations (Cross *et al.*, 2014; Wang *et al.*, 2016; Kim *et al.*, 2012; Oxnard *et al.*, 2011; Walter *et al.*, 2013; Chong *et al.*, 2013). Most of them are still far from being used clinically due to their relatively weak binding activity to the EGFRs or severe toxicity (Thress *et al.*, 2015; Gazdar, 2009). Mutant EGFRs with the T790M mutations direct more robust downstream signalling, via pathways such as **PI3K/Akt/mTOR, IL-6/STATs**, and **Wnt/ β -catenin** (Kim *et al.*, 2012; Terai *et al.*, 2013; Zhang *et al.*, 2012; Gao *et al.*, 2007; Wangari-Talbot *et al.*, 2013; Stewart *et al.*, 2015). In addition, many pro-oncogenes and anti-oncogenes are aberrantly expressed in NSCLC with the EGFR T790M mutation. Thus, these genes could be novel drug targets for the therapy of T790M-containing NSCLC.

The cancer/testis antigens (CTAs) are a group of tumour-associated antigens (TAAs), which display normal expression in the adult testis, an immune-privileged organ. However, they display aberrant expression in several types of cancers, particularly in advanced cancers with stem cell-like characteristics (Kulkarni *et al.*, 2012; Kalejs *et al.*, 2005; Old, 2001). There has been an explosion in CTA-based research since CTAs were first identified in 1991 and MAGE-1 was shown to elicit an autologous cytotoxic T-lymphocyte (CTL) response in a patient with melanoma (Kulkarni *et al.*, 2012; Kalejs *et al.*, 2005; Old, 2001). The resulting data have not only highlighted a role for CTAs in tumourigenesis but have also underscored the translational potential of these antigens for detecting and treating many types of cancers. Due to their increased specificity and sensitivity compared to those currently used clinically, studies have indicated that these CTAs have potential roles as novel biomarkers in cancer immunotherapy (Kulkarni *et al.*, 2012; Kalejs *et al.*, 2005; Old, 2001; Odunsi *et al.*, 2003).

Pentacyclic triterpenoids naturally occur in a wide variety of plants and exhibit a number of biological activities, including the induction of apoptosis, autophagy, anti-inflammation and antineoplastic activity (Laszczyk, 2009; Xiang *et al.*, 2015). Pentacyclic triterpenoids mainly comprise the oleananes, ursanes, lupanes, and friedelanones (Laszczyk, 2009). The representatives of the four types of compounds are **oleanolic acid**, glycyrrhetic acid, ursolic acid (UA), asiatic acid (AA, 23-hydroxybetulinic acid), and tripterone (Laszczyk, 2009; Xiang *et al.*, 2015). Among them, UA was frequently reported to have anti-cancer effects on a variety of malignant tumours, including breast cancer, leukemia, prostate cancer, lung cancer, melanoma, and liver cancer (Novotny *et al.*, 2001; Shanmugam *et al.*, 2013; Shanmugam *et al.*, 2011; Kim *et al.*, 2015; Kashyap *et al.*, 2016; Kim *et al.*, 2014; Zhang *et al.*, 2016), suggesting its potential application in clinical cancer treatment. There are several underlying anti-tumour mechanisms for UA, including the

What is already known

- EGFR T790M mutation leads to resistance to most clinically available EGFR tyrosine kinase inhibitors.
- For lung cancer with EGFR T790M mutations, there are few clinically effective chemotherapy drugs.

What this study adds

- CT45A2 is highly expressed in NSCLC with EGFR T790M mutations and may increase resistance.
- Ursolic acid inhibits NSCLC with EGFR T790M mutations by suppressing CT45A2 expression.

Clinical significance

- Ursolic acid could be used in the treatment of NSCLC harbouring EGFR T790M mutations.

activation of **c-Jun N-terminal kinase (JNK)**, Ca^{2+} release, suppression of NF- κ B, and the **signal transduction and activation of transcription-3 (STAT-3)**, and β -catenin (Shanmugam *et al.*, 2011; Kim *et al.*, 2015; Kashyap *et al.*, 2016; Kim *et al.*, 2014; Zhang *et al.*, 2016). However, whether UA has anti-cancer effect on NSCLC carrying the EGFR T790M mutation remains unknown. In this study, we have described that, among pentacyclic triterpenoids, UA had the greatest inhibitory effect on the growth of NSCLC tumours carrying the EGFR T790M mutation. Further, the anti-cancer effect of UA was largely dependent on CT45A2 and that UA inhibited CT45A2 expression at transcriptional level. The results in this study highlight the importance of UA in the therapy of NSCLC with the T790M mutation in EGFRs.

2 | METHODS

2.1 | Cell lines

Human NSCLC cell lines A549 (NCI-DTP Cat# A549, RRID: CVCL_0023), H1299 (NCI-DTP Cat# NCIH1299, RRID:CVCL_0060), HCC827 (EGFR exon 19 deletion [delE746-A750]), and H1975 (L858R-T790M) cells were obtained from the American Type Culture Collection (Manassas, VA, USA). HCC827 and H1975 cells were cultured in RPMI-1640 medium (Wisent Corporation, Wisent, Canada) supplemented with 10% FBS (Thermo Scientific, HyClone Laboratories Inc., Logan, UT, USA) and penicillin (100 U·ml⁻¹)/streptomycin (100 μ g·ml⁻¹; Wisent Corporation). The other cells were cultured in DMEM (Wisent Corporation) supplemented with 10% FBS (Thermo Scientific, HyClone Laboratories Inc.) and penicillin (100 U·ml⁻¹)/streptomycin (100 μ g·ml⁻¹; Wisent Corporation). All cell lines were cultured in a humidified incubator with 5% CO₂ at 37°C.

2.2 | siRNA transfection

The siRNAs against CT45A2 (si-CT45A2) were used to knock down endogenous CT45A2 expression. A scrambled siRNA (si-NC) was used as a negative control. The siRNA sequences listed in Table S1 were designed and synthesized by GenePharma Co., Ltd (Shanghai, China). H1975 cells were plated in RPMI1640 at a density of 1.0×10^4 cells·ml⁻¹ in 24-well plates. At approximately 50% confluence, cells were transfected with 200 nmol·L⁻¹ of siRNA in lipofectamine 2000 reagent (Invitrogen, Carlsbad, CA, USA) according to the manufacturer's instructions. Briefly, 4- μ l lipofectamine 2000 was diluted in 200- μ l Opti-MEM (Life Technologies, Gaithersburg, MD, USA) and incubated for 5 min at room temperature. In a separate tube, 4 μ l of 50 μ mol·L⁻¹ of siRNA was diluted in 200 μ l of Opti-MEM. Diluted oligofectamine reagent (200 μ l) was added to the diluted siRNA solution, and the complex was incubated for 20 min at room temperature. siRNA + Opti-MEM complexes (400 μ l) were added to each dish/well. The final concentration of the siRNA was 200 nmol·L⁻¹. After 8 hr, fresh RPMI1640 containing 10% FBS was added. At 36 hr after the initiation of transfection, cells were harvested for RT-PCR or treated with UA. Western blot was performed after the transfected cells were cultured for 48 hr.

2.3 | Plasmid construction

The coding sequence of human CT45A2 was cloned into a FLAG-tagged pRK5 mammalian expression vector. To construct plasmids with firefly luciferase as a reporter gene directed by the human CT45A2 promoter, a BglII/Xho-1 digest of CT45A2 PCR product (2,050 bp) and their variants were subcloned into pGL3-basic vector (Promega, Madison, WI, USA). All primer pairs are provided in Tables S2 and S3.

2.4 | Cell viability assays

Cells were seeded in 100 μ l culture medium in 96-well plates at a density of 4,000 cells per well. After treatments, 10 μ l of 5 mg·ml⁻¹ of thiazolyl blue tetrazolium bromide (3-(4,5-dimethylthiazol-2-yl)-2,5-diphenyl tetrazolium bromide [MTT]; Ameresco Co., Solon, OH, USA) in PBS was added, and the culture plates were further incubated at 37°C for 2 hr. The MTT solution was aspirated, and DMSO solution was added and incubated at room temperature for 5 min. The absorbance was read on a spectrophotometer (Elx800, BioTEK instrument, USA) at 490 or 570 nm. Cell viability was calculated as the following ration: cell viability = $OD_{\text{sample}}/OD_{\text{control}} \times 100\%$. OD_{sample} is the A_{490} or A_{570} of each group with UA, [erlotinib](#), CT45A2-pRK5, or CT45A2 siRNA treatment, and OD_{control} is the A_{490} or A_{570} of empty vector, scrambled siRNA, or the untreated group. The results shown are the means \pm SD from five independent experiments.

2.5 | Wound healing assays

H1975 cells were cultured in RPMI1640 medium supplemented with 10% FBS, seeded into 24-well plates at a density of 5.0×10^4 cells·ml⁻¹. After 30–40% confluence, cells were transfected with CT45A2-pRK5-Flag or CT45A2 siRNA to overexpress or knock down CT45A2 protein expression. After 24 hr, scratches were made using 100- μ l pipette tips, and the wells were washed twice with medium with 2% FBS. Cells were treated with UA or allowed to grow for an additional 24, 48, and 72 hr. The gap distance was quantitatively measured by using ImageJ software (ImageJ, RRID: SCR_003070).

2.6 | Annexin V-FITC/propidium iodide apoptosis assay

Apoptotic rates were analysed by flow cytometry using a commercially available Annexin V-FITC/propidium iodide (PI) apoptosis detection kit (KeyGen, Nanjing, China). Staining was performed according to the manufacturer's instruction, and flow cytometry was conducted on a BD Accuri C6 flow cytometer (BD Biosciences, San Jose, USA). In this assay, Annexin V⁺/PI⁻ populations are early apoptotic cells, and Annexin V⁺/PI⁺ populations are late apoptotic (secondary necrotic form) and primary necrotic cells. Flow cytometry data are from five independent experiments.

2.7 | Luciferase reporter assays

H1975 cells (1.0×10^4 cells per well) were plated in 24-well plates 24 hr before transfection. The pGL3-CT45A2-Luc, an internal standard plasmid pRL-SV40 (Promega), and control vector pGL3-basic were co-transfected into H1975 cells with the use of PolyJet reagent (#SL100688, SignaGen, MD, USA). The next day, the medium was changed, and DMSO or UA (25 μ mol·L⁻¹) was added. Twelve hours later, measurements of firefly and *Renilla* luciferase activities in cell lysates were carried out with the use of the Dual-Luciferase Reporter Assay System according to the manufacturer's instructions (Promega). Data were presented as the ratio of firefly luciferase activity to *Renilla* luciferase activity in each sample performed in triplicate. Data are expressed as means \pm SD from five independent experiments.

2.8 | Chromatin immunoprecipitation assay

H1975 cells were fixed with 1% formaldehyde at 37°C for 10 min and subsequently washed twice with ice-cold PBS containing protease inhibitors. Cells were incubated in a lysis buffer (1% SDS, 10 mmol·L⁻¹ of EDTA, 50 mmol·L⁻¹ of Tris-HCl, pH 8.1) for 10 min on ice and sonicated to shear genomic DNA. The lysate was centrifuged for 10 min at 16,000 \times g at 4°C. The supernatant was diluted in a chromatin

immunoprecipitation (ChIP) dilution buffer (0.01% SDS, 1% Triton X-100, 2 mmol·L⁻¹ of EDTA, 16.7 mmol·L⁻¹ of Tris-HCl, pH 8.1, 167 mmol·L⁻¹ of NaCl, and protease inhibitors). Anti-TCF4 (Thermo Fisher Scientific Cat# MA5-11184, RRID:AB_10980560) or IgG (negative control) antibodies were added to the supernatant and incubated overnight at 4°C with rotation. Protein A agarose slurry was added and incubated at 4°C for 1 hr with constant rotation. Agarose beads were collected by centrifugation and washed, and antibody-bound chromatin was released from the agarose beads. DNA was purified by phenol/chloroform extraction and isoamyl alcohol precipitation. Binding was detected by PCR.

2.9 | RT-PCR and real-time quantitative PCR

Total RNA was extracted, from harvested cells, using Trizol reagent (Sangon Biotech, Shanghai, China) according to the manufacturer's instructions. First-strand cDNA was synthesized from total RNA using PrimeScript RT Master Mix (#RR036A, Takara, Dalian, China). Amplification of specific PCR products was detected using 2× TSINGKE Master Mix (TSINGKE Biological Technology, Beijing, China) according to the manufacturer's instructions. The PCR products were separated by electrophoresis on 1.0% agarose gels containing GelRed along with DNA markers. GAPDH was used as an internal control. Real-time quantitative PCR was performed with an ABI StepOne Plus (Applied Biosystems, Foster City, CA, USA) using 2× SYBR green PCR mixture (Bio-Rad, Hercules, CA, USA) according to the manufacturer's instructions. Data were normalized by the β-actin mRNA level. Data shown are from five independent experiments. The specific primer sequences are listed in Supplementary information (Table S4)

2.10 | Western blot and immunofluorescence

For western blot analysis, cells were washed with PBS and lysed on ice with RIPA supplemented with a protease inhibitor cocktail (Roche Diagnostics). Lysates were analysed by SDS-PAGE followed by blotting with the indicated antibodies. Antibodies against the following proteins were used: β-catenin (1:2,000), glycogen synthase kinase (GSK)-3β (1:1,000), p-β-catenin (Ser^{33/37}/Thr⁴¹; 1:2,000), p-GSK-3β (Ser⁹; 1:1,000), TCF4 (1:1,000), and GAPDH (1:5,000). HRP-conjugated anti-mouse and anti-rabbit antibodies were used, respectively. The signal was detected using an enhanced chemiluminescence system (Cell Signaling Technology, Beverly, MA, USA). The results of protein expression are normalized to GAPDH. The blots shown are representative of five independent experiments.

For immunofluorescence analysis, the H1975 cells after UA treatments on coverslips were fixed with 4% paraformaldehyde and permeabilized by PBS containing 0.1% Triton X-100, blocked with 5% BSA for 1 hr at 37°C, and incubated with the β-catenin antibody (1:200) at 4°C overnight. Then cells were washed with PBS and incubated with Alexa Fluor 488-conjugated secondary antibodies (1:600,

Abcam, Cambridge, UK) for 1 hr at 37°C. Nuclear staining was achieved by incubating the cells in Hoechst33342 for 10 min. The fluorescence was photographed with fluorescence microscopy (NEXCOPE930, Nexcope, USA).

2.11 | Mouse xenograft model and immunohistochemical analysis

All animal care and experimental procedures complied with the University's Guidelines for the Care and Use of Laboratory Animals. Animal studies are reported in compliance with the ARRIVE guidelines (Kilkenny, Browne, Cuthill, Emerson, & Altman, 2010). Thirteen 3-4-week-old male athymic nude mice were purchased from the Model Animal Research Center of Nanjing University (Nanjing, China). The mice were housed in a temperature-(22-25°C), humidity-(40-60%) and light-(12h dark/light) controlled environment and fed with standard chow and water.

To establish the xenograft model, H1975 cells (5×10^6) were inoculated subcutaneously on the flanks of the athymic nude mice. When the average tumour size reached ~100 mm³, mice with tumour xenografts were randomized into three groups: (1) vehicle group (normal saline with 1% DMSO) with five mice, (2) UA group (25 mg·kg⁻¹) with five mice, and (3) erlotinib group (20 mg·kg⁻¹) with three mice. All of the treatments were injected once a day for 18 days. The formula, (length × width²)/2, was used to estimate tumour sizes. Tumour sizes were recorded once every 2 days. At the end of the experiment, the animals were killed, and the tumours were dissected and weighed.

Paraffin tissue sections were obtained from the tumour tissues from the nude mice and immunohistochemical analyses were performed as described previously (Walter et al., 2013). The antibody-based procedures used in this study comply with the recommendations made by the *British Journal of Pharmacology*. Briefly, the sections were deparaffinized with xylene and rehydrated with gradients of ethanol (100%, 95%, and 70%). After quenching the endogenous peroxidases with 3% hydrogen peroxide, the sections were microwaved for 10 min in the presence of 10 mmol·L⁻¹ of citric acid buffer and blocked by 5% BSA/0.3% Triton X-100 for 20 min. Then the sections were incubated with cleaved caspase-3 (1:200) antibody overnight at 4°C. Following overnight incubation, slides were rinsed and incubated with a horseradish-conjugated secondary antibody (1:1,000) for 30 min at 37°C, and then signal was generated by using the DAB substrate kit (Boster, Wuhan, China). The sections were observed under optical microscope (NEXCOPE930, Nexcope).

2.12 | Haematoxylin-eosin staining and TUNEL staining

Liver and kidney tissues from mice were embedded in paraffin blocks and subjected to haematoxylin and eosin (H&E) staining. Briefly, sections were deparaffinized in xylene and rehydrated with gradients of

ethanol (100%, 95%, 80%, and 70%). They were then stained with haematoxylin for 10 min, rinsed with 1% hydrochloric acid alcohol for 2 s, rinsed with tap water for 15 min, stained with eosin for 2 min, and rinsed again with distilled water. The slides were then dehydrated with 95% and 100% ethanol successively followed by xylene and mounted with coverslips. The TUNEL assay was used to assess apoptosis and assays was performed according to the manufacturer's instructions (TUNEL Apoptosis Assay Kit, KeyGEN, Nanjing, China). Specimens were examined by light microscopy (NEXCOPE930, Nexcope).

2.13 | Data and statistical analysis

The data and statistical analysis in this study complied with the recommendations on experimental design and analysis in pharmacology (Curtis *et al.*, 2018). Data are presented as mean \pm SD unless otherwise specified. Results were obtained from five independent experiments. Statistical analysis was performed with one-way ANOVA followed by Tukey's post-hoc test when comparing multiple independent groups, and when comparing two different groups, the unpaired t-test was carried out. Post-hoc tests were run only if F achieved $P < 0.05$ and there was no significant variance inhomogeneity. A P-value of < 0.05 was considered statistically significant.

2.14 | Materials

UA, AA, GA and OA (purity $\geq 98\%$ by HPLC) was purchased from Shanghai Yuanye Biotechnology Company (Shanghai, China), Erlotinib was purchased from Natco pharma Ltd. (Hyderabad, India). Complete protease inhibitor cocktail tablets from Roche Diagnostics (Mannheim, Germany), and RIPA from Biyuntian (Shanghai, China). Protein A/G PLUS-Agarose (sc-2003) was purchased from Santa Cruz Biotechnology (Santa Cruz, CA, USA). Antibodies to detect total GSK-3 β (22104-1-AP) and total β -catenin (51067-2-AP) and T-cell factor 4 (TCF4; 22337-1-AP) were purchased from Proteintech Co., (Wuhan, China). Phosphorylated GSK-3 β (Ser⁹; AF2016) and phosphorylated β -catenin (Ser^{33/37}/Thr⁴¹; DF2989) were purchased from Affinity Biosciences (Shanghai, China). The antibody to detect GAPDH (AP0063) was purchased from Bioworld Biotechnology (Nanjing, China).

2.15 | Nomenclature of targets and ligands

Key protein targets and ligands in this article are hyperlinked to corresponding entries in <http://www.guidetopharmacology.org>, the common portal for data from the IUPHAR/BPS Guide to PHARMACOLOGY (Harding *et al.*, 2018), and are permanently archived in the Concise Guide to PHARMACOLOGY 2019/20 (Alexander, Fabbro *et al.*, 2019aa, 2019bb; Alexander, Kelly *et al.*, 2019).

3 | RESULTS

3.1 | UA inhibited cell proliferation and motility in H1975 cells harbouring EGFR L858R/T790M mutation

To evaluate the efficacy of **erlotinib** in vitro, cell proliferation was assessed in human NSCLC cell lines, with the MTT assay. Among these cell lines, both A549 and H1299 have wild-type EGFR, HCC827 cells harbour the EGFR (delE746-A750) mutation, and H1975 cells harbour the EGFR L858R/T790M mutation. Cells were treated with erlotinib for 48 hr at $5 \mu\text{mol}\cdot\text{L}^{-1}$. As shown in Figure 1A, erlotinib significantly reduced HCC827 cells viability but had no effects on H1975 cells and other cells with wild-type EGFR, suggesting that H1975 cells with the T790M mutation are relatively resistant to erlotinib treatment. Given this fact, H1975 cells were used in subsequent experiments.

The pentacyclic triterpenoids are naturally occurring compounds that have strong anticancer activities. To examine whether these compounds could be beneficial for the treatment of NSCLC with the T790M mutation, we examined the effects of oleanolic acid, glycyrrhetic acid, UA and AA on the viability of H1975 cells. As shown in Figure 1b, of these pentacyclic triterpenoids, only UA and AA significantly suppressed the growth of H1975 cells, and in a dose-dependent manner (Figure 1c). As a negative control, erlotinib showed no effect on viability (Figure 1b,c). Previous studies have shown that UA was less toxic than AA to normal cells (Salvador *et al.*, 2017; Vo, Fukushima, & Muranaka, 2017). Consistent with these findings, we found that UA had lower toxicity than AA in human normal lung epithelial (BEAS-2B) cells (Figure 1d). Interestingly, UA and AA had no inhibitory effect on EGFR-mutant HCC827 cells but significantly inhibited EGFR wild-type A549 and H1299 cells (Figure S1). For patients with EGFR wild-type lung cancer, chemotherapy, with drugs such as **paclitaxel** and **oxaliplatin**, is more effective than treatment with EGFR-TKIs such as erlotinib. However, for patients with lung cancers with the EGFR T790M mutant, there are currently few clinically effective chemotherapy drugs for its treatment. Therefore, we investigated the mechanism underlying the effects of UA on H1975 cells which harbour the EGFR L858R/T790M mutation. Annexin V-FITC/PI assays showed that UA induced apoptosis in H1975 cells (Figure 1e) and inhibited cell motility in wound healing assays with the H1975 cells (Figure 1f).

3.2 | UA suppresses tumour growth and induces apoptosis in vivo

To assess whether the effect of UA on H1975 cells growth also occurs in vivo, we established the xenograft mice model by subcutaneous injections of erlotinib-resistant H1975 cells into the flanks of athymic nude mice. When the tumours reached 100–250 mm³ in volume, the mice were challenged with either the vehicle (DMSO), UA ($25 \text{ mg}\cdot\text{kg}^{-1}\cdot\text{day}^{-1}$), or erlotinib ($20 \text{ mg}\cdot\text{kg}^{-1}\cdot\text{day}^{-1}$) for 18 days. The

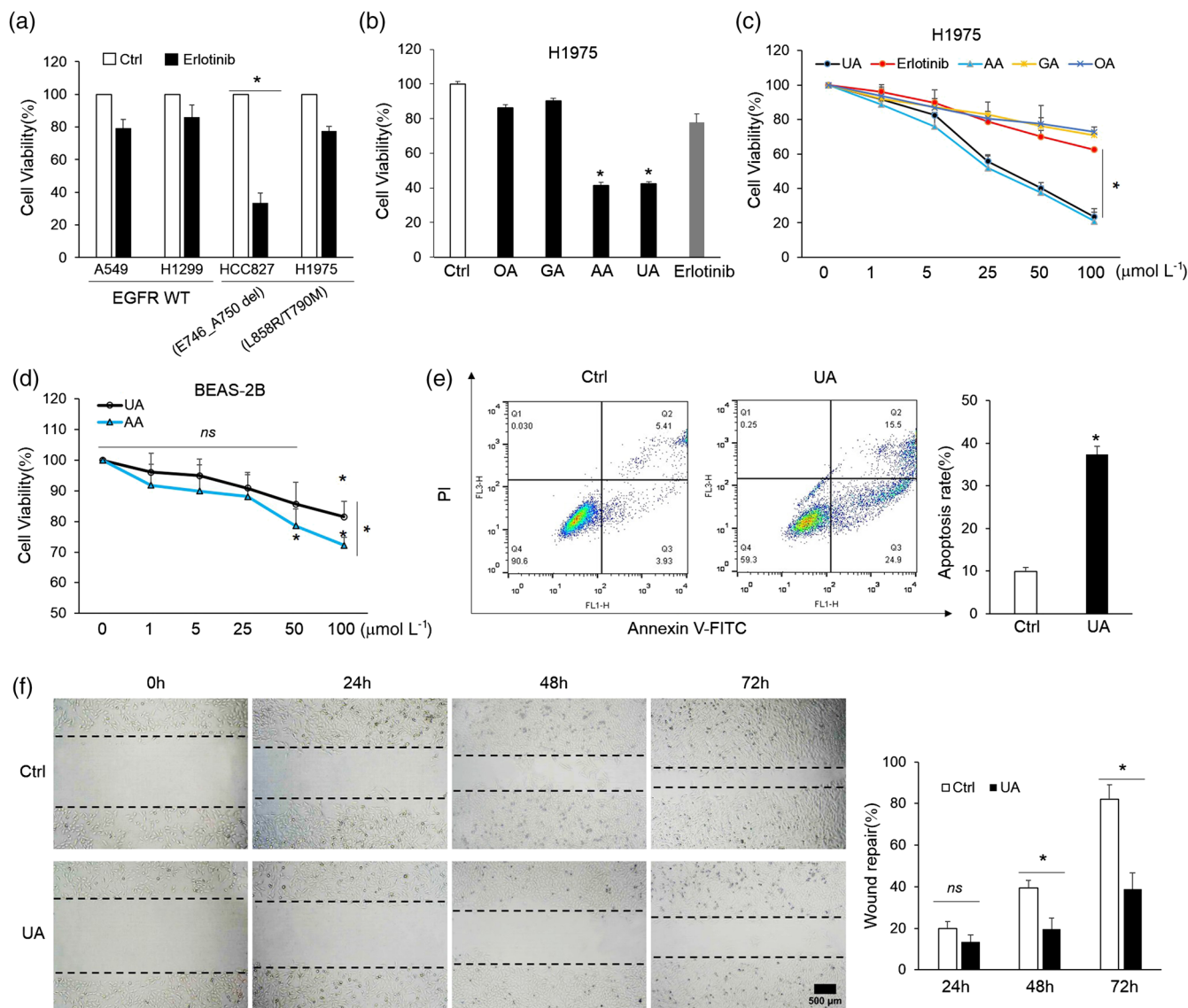


FIGURE 1 Ursolic acid inhibited cell proliferation and motility in H1975 cells harbouring the EGFR L858R/T790M mutation. (A) H460, H1299, HCC827, and H1975 cells were incubated with $5 \mu\text{mol L}^{-1}$ of erlotinib for 48 hr and cell viability was analyzed using by MTT assay. (B) H1975 cells were treated with oleanolic acid (OA, $50 \mu\text{mol L}^{-1}$), glycyrrhetic acid (GA, $50 \mu\text{mol L}^{-1}$), ursolic acid (UA, $50 \mu\text{mol L}^{-1}$), asiatic acid (AA, $50 \mu\text{mol L}^{-1}$) and erlotinib ($5 \mu\text{mol L}^{-1}$) for 48 hr. Cell viability was measured by MTT assay at an absorbance of 490 nm. (C) H1975 cells were treated with different concentrations of UA, AA, GA, OA and erlotinib for 48 hr. Cell viability was measured by MTT assay at an absorbance of 490 nm. (D) Cytotoxic effects of different concentrations of UA and AA on human normal lung epithelial (BEAS-2B) cells. Cell viability was analyzed using by MTT assay. (E) H1975 cells were treated with UA ($25 \mu\text{mol L}^{-1}$) and then stained with AnnexinV-FITC and propidium iodide for detecting apoptosis by flow cytometry. (F) H1975 cells were treated with UA ($25 \mu\text{mol L}^{-1}$) for different times (24,48,72 hr), changes in cell motility were assessed by scratch wound healing assay. Scale bar=500 μm . Data shown are means \pm SD from five independent experiments ($n = 5$). * $P < 0.05$, significantly different as indicated; ns, non-significant effects

results demonstrated that UA treatment retarded the growth of H1975 tumour xenografts (Figure 2a,b) and also decreased tumour weight (Figures 2c and S2). Surprisingly, although H1975 cells were resistant to erlotinib treatment in vitro, the results of in vivo experiments indicated that erlotinib had a weak inhibitory effect on H1975 tumour growth (Figure 2a-c). The antitumour effects of UA in vivo were also confirmed by TUNEL staining assay (Figure 2d). As shown

in this figure, UA treatment increased TUNEL-positive cells in tumour tissue, compared to the control group. In the erlotinib treatment group, TUNEL-positive cells were also higher than that in the control group but this effect was less marked than that of UA. We subsequently conducted histological evaluations of UA toxicity in the liver and kidneys. Haematoxylin and eosin staining indicated that UA had no toxic effects on either the kidney or liver tissue (Figure 2e),

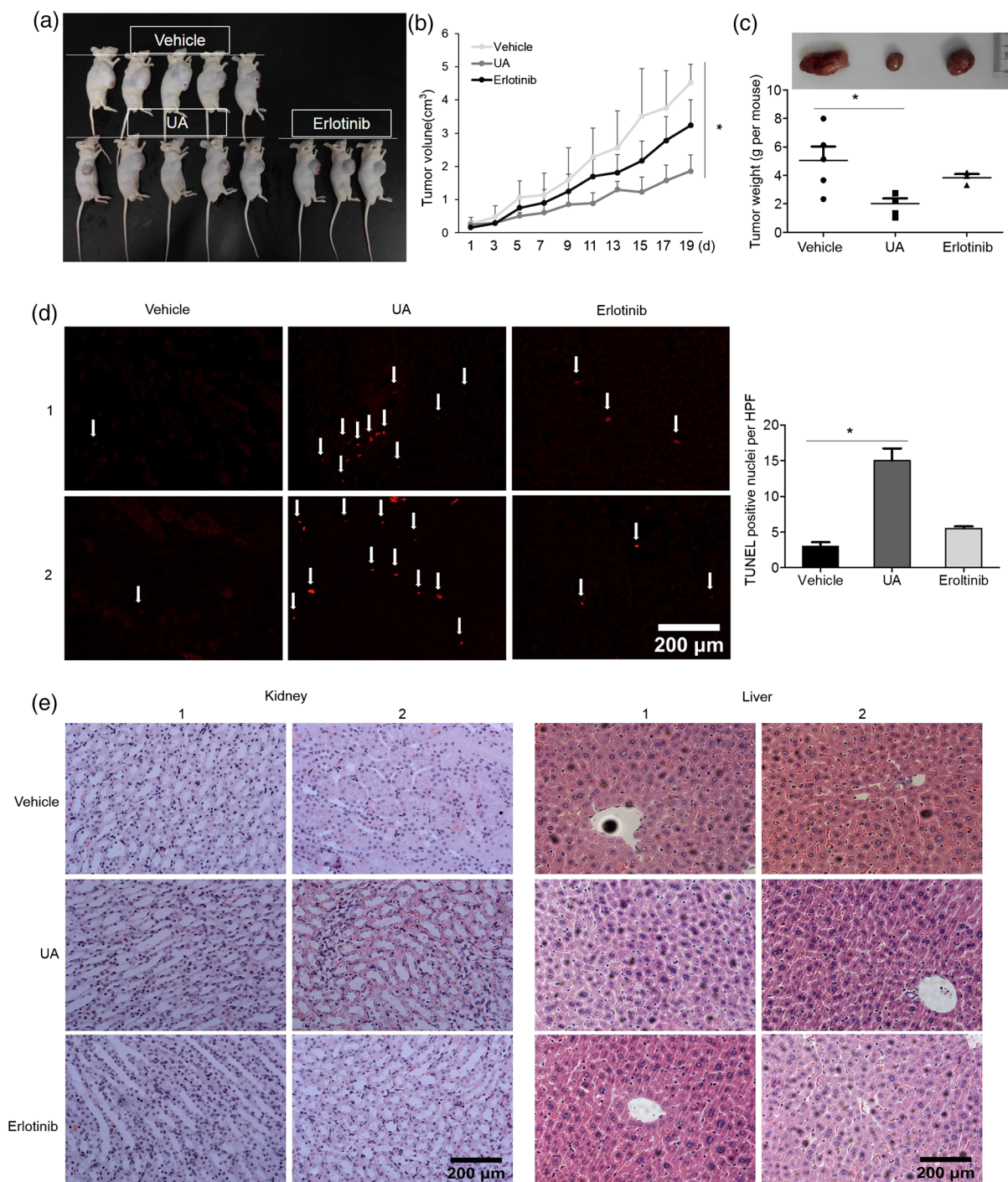


FIGURE 2 Ursolic acid (UA) suppressed xenograft tumour growth and induced apoptosis in vivo. (A) H1975 cells were injected subcutaneously into the dorsal right flank of athymic nude mice. Mice were injected with UA (25 mg kg⁻¹ day⁻¹) or vehicle (normal saline with 1% DMSO) or erlotinib (20 mg kg⁻¹ day⁻¹) once a day for 18 days. Mice were killed and tumour tissues collected. Photographs of mice and tumours from each treatment group taken at autopsy. (B) Tumour volume was calculated from measurements of 2 diameters of the individual tumour based on the following formula: tumour volume (mm³) = (length × width² × 0.5). Data shown are means ± SE of values obtained from the experiments. **P* < 0.05, significantly different as indicated. (C) Up: representative tumour example is shown. Down: Weights of the tumours per mouse. Data shown are means ± SEM. **P* < 0.05. (D) Left: Tumour samples derived from H1975 xenografts were retrieved, fixed and paraffin embedded. Sections were used for examining apoptotic cells by TUNEL staining. White arrows indicate TUNEL-positive cells with characteristic apoptotic morphology. Representative images are shown. Scale bar=200 μm. Right: Analysis and statistics of TUNEL staining results in Fig 2D left. The number of TUNEL-positive cells were quantified from 5 high-power fields (HPF). (E) The degrees toxicity in liver and kidney samples were evaluated by light microscopy after H&E staining. Representative images are shown. Scale bar=200 μm. Data shown are means ± SD from five independent experiments for the vehicle group and the UA group; three independent experiments for the erlotinib group. **P* < 0.05, significantly different as indicated

suggesting that UA at 25 mg·kg⁻¹·day⁻¹ as used in this study, was relatively safe *in vivo*.

3.3 | CT45A2 was highly expressed in H1975 cells harbouring EGFR L858R/T790M

To explore whether lung cancer harbouring EGFR T790M displays additional new activation genes which may play a role in disease progression. We performed gene expression omnibus (GEO) dataset analysis of the sensitivity of NSCLC cell lines to gefitinib (<https://www.ncbi.nlm.nih.gov/geo/gds/analyze/analyze.cgi?ID=GDS2298>).

Gefitinib is another EGFR TKI. The analysis revealed that many genes, including ZDHHC24, EREG, RAP2B, GNA12, EGLN1, CT45A2, and TMEM18, were highly expressed in gefitinib-resistant H1975 cells, when compared with those cells with the EGFR (DeLE746–E750) or EGFR L858R mutations (Figures 3a and S3A). Among these genes, that for CT45A2 (also known as CT45A8) had the highest expression (<https://www.ncbi.nlm.nih.gov/geo/profiles/29756486>; Figure S3B).

Consistent with this result, the results of QPCR also confirmed that CT45A2 mRNA levels were higher than those for other genes (Figure 3b). We therefore investigated the role of CT45A2 in NSCLC with the EGFR T790M mutation. The full length of CT45A2 cDNA was amplified and cloned into pRK5 expressing vector, which was transfected into H1975 cells (Figure 3c). As a result, the forced CT45A2 expression led to increased proliferation of the H1975 cells, as assessed by MTT assay. Such overexpression of CT45A2 also significantly accelerated wound healing (Figure 3d). On the contrary, silencing of CT45A2 expression in the H1975 cells inhibited cell growth (Figure 3e) and retarded the wound healing (Figure 3f). Taken together, CT45A2 positively regulated the proliferation and motility of H1975 cells *in vitro*.

3.4 | CT45A2 is required for UA-induced H1975 cell apoptosis

To examine whether the anticancer effect of UA was dependent on CT45A2, H1975 cells after transfection with CT45A2 were exposed to UA treatment. We found that the suppressive effect of UA on H1975 cells growth was greatly attenuated in cells overexpressing CT45A2 (Figure 4a), suggesting that the effect of UA was probably dependent on CT45A2. To confirm this dependence, CT45A2 expression in H1975 cells was silenced and the cells then treated with UA. MTT assay demonstrated that either CT45A2 expression knockdown or UA treatment alone inhibited the proliferation of H1975 cells. However, when CT45A2-silenced cells were treated with UA, UA failed to augment the inhibition of cell proliferation (Figure 4b). Notably, UA failed to increase the sensitivity of H1975 cells to erlotinib (Figure S4). Annexin V-FITC/PI assays showed that UA-induced apoptosis in H1975 cells was attenuated by CT45A2 silencing (Figure 4c). Therefore, CT45A2 appeared to be critically involved in the pro-apoptotic effect of UA on H1975 cells.

3.5 | UA inhibited the CT45A2 gene promoter through TCF4 sites in H1975 cells

Among genes that were up-regulated in gefitinib-resistant H1975 cells, UA was found to inhibit the mRNA expression of CT45A2 but not other genes, as examined by semiquantitative (Figure 5a) or quantitative RT-PCR analysis in the H1975 cells (Figure 5b). We therefore hypothesized that UA may suppress CT45A2 gene expression at the level of mRNA transcription or mRNA decay. To test this hypothesis, we used actinomycin D (4 µg·ml⁻¹) to halt all gene transcription and then observed the mRNA half-life of CT45A2 in H1975 cells after UA treatment (Figure 5c). The results demonstrated that UA failed to influence the half-life of CT45A2 mRNA (Figure 5c,d). Therefore, UA-mediated down-regulation of CT45A2 most likely occurred at the level of transcription.

To evaluate the effects of UA on CT45A2 gene transcription, we cloned the full length of human CT45A2 promoter and its truncated variants (–2,000 to +50, into pGL3 reporter construct). The results, as shown in Figure 5e, indicated that UA significantly suppressed the luciferase activity of the full-length CT45A2 promoter in H1975 cells. To identify the potential *cis*-elements involved in the effect of UA on CT45A2 gene transcription, truncated variants of full-length CT45A2 promoter (–1,000 to +50, –600 to +50, –300 to +50, –180 to +50, and –100 to +50 bp) were constructed, and the result demonstrated that UA-mediated suppression on CT45A2 promoter activity was completely abolished in the truncated variant containing –180 to +50 bp, suggesting that the UA-responsive *cis*-element may exist in the sequence between –300 and –180 bp of the CT45A2 promoter. Bioinformatic analysis revealed that there is a putative TCF4 binding site within this region (–300 to –180; Figure 5f; http://algggen.lsi.upc.es/cgi-bin/promo_v3/promo/promoinit.cgi?dirDB=TF_8.3). We thus constructed deletion mutations in specific TCF4 binding sites to detect CT45A2 promoter luciferase activity in H1975 cells. Results in Figure 5g showed that UA failed to down-regulate CT45A2 gene promoter luciferase activity when the TCF4 binding site was mutated. Similar results were also observed in H1975 cells when TCF4 expression in H1975 cells was silenced (Figure 5h). In parallel, ChIP assays also confirmed that lysates from UA treated with H1975 cells exhibited decreased binding to CTTTGTA sequences (Figure 5i). These results revealed that UA decreased CT45A2 mRNA expression by preventing TCF4 binding on the promoter.

3.6 | UA inhibited the β-catenin/TCF4 signalling pathway in vitro and in vivo

As UA decreased TCF4 binding at the CT45A2 promoter; we investigated whether TCF4 was involved in the inhibition of CT45A2 mRNA level by UA. H1975 cells with or without transfection with siNC or siTCF4 were exposed to UA and semi-quantitative PCR carried out. The results demonstrated that CT45A2 mRNA levels were significantly reduced after silencing TCF4. Moreover, the inhibition of CT45A2 gene expression by UA was greatly attenuated after TCF4

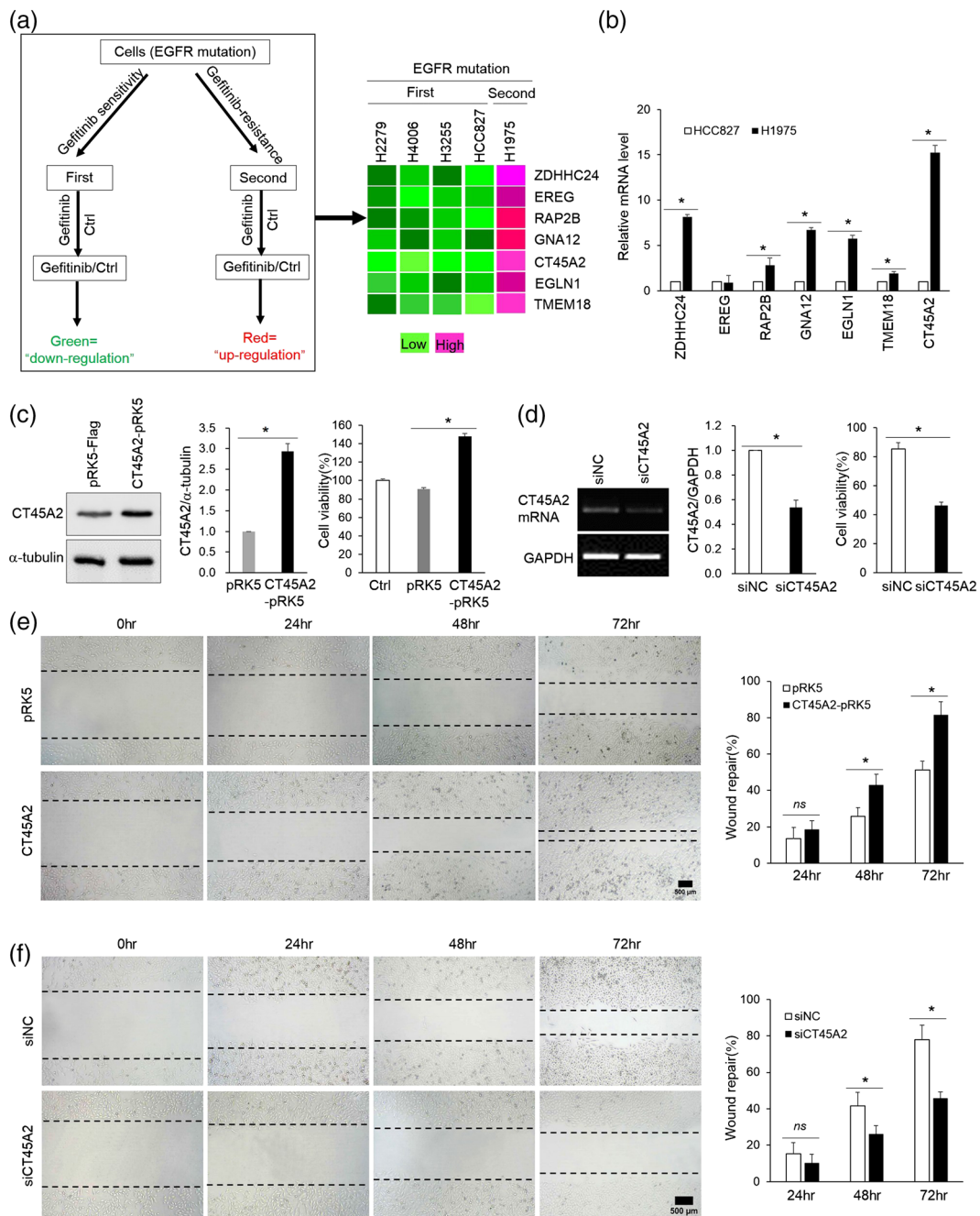


FIGURE 3 CT45A2 was highly expressed in H1975 cells harbouring the EGFR L858R/T790M mutation. (A) Analysis of baseline non-small cell lung cancer (NSCLC) cell lines with a broad range of sensitivity to the anticancer drug gefitinib. GEO datasets results were used to define gene expression signature of gefitinib sensitivity. Gefitinib effect on various NSCLC lines (HG-U133B). (<https://www.ncbi.nlm.nih.gov/geo/gds/analyze/analyze.cgi?ID=GDS2298&dist=1&method=2&geneBegin=7169&geneToGet=3542&PC=5&NC=1&action=1>). Genes including ZDHHC24, EREG, RAP2B, GNA12, EGLN1, CT45A2, and TMEM18 were highly expressed in gefitinib-resistant H1975 cells. (B) The total RNA of HCC827 and H1975 cells was extracted, and Q-PCR was performed to examine the mRNA level of the indicated genes (ZDHHC24, EREG, RAP2B, GNA12, CT45A2). The endogenous GAPDH RNA was used as the internal control. (C) H1975 cells were transfected with CT45A2-overexpressing plasmid, and the cell viability was measured by MTT assay. The indicated proteins were detected by western blotting. The middle graph shows the mean values from western blotting. Protein levels were quantified using gray value analyses by Image J software. (D) H1975 cells were transfected with siRNA against CT45A2 (siCT45A2) or a negative control siRNA (siNC), the indicated gene was detected by PCR. The middle graph shows the mean values from PCR. CT45A2 mRNA level was analyzed by Image J software. Cell viability was evaluated using by MTT assay. (E) H1975 cells were transfected with CT45A2-overexpressing plasmid, and the cell motility was investigated using wound-healing assay. Scale bar=500 μm. (F) H1975 cells were transfected with siCT45A2 or siNC. Cell motility was evaluated using by wound healing assay. Scale bar=500 μm. Data shown are means ± SD from five independent experiments *P < 0.05, significantly different as indicated; ns, non-significant effects

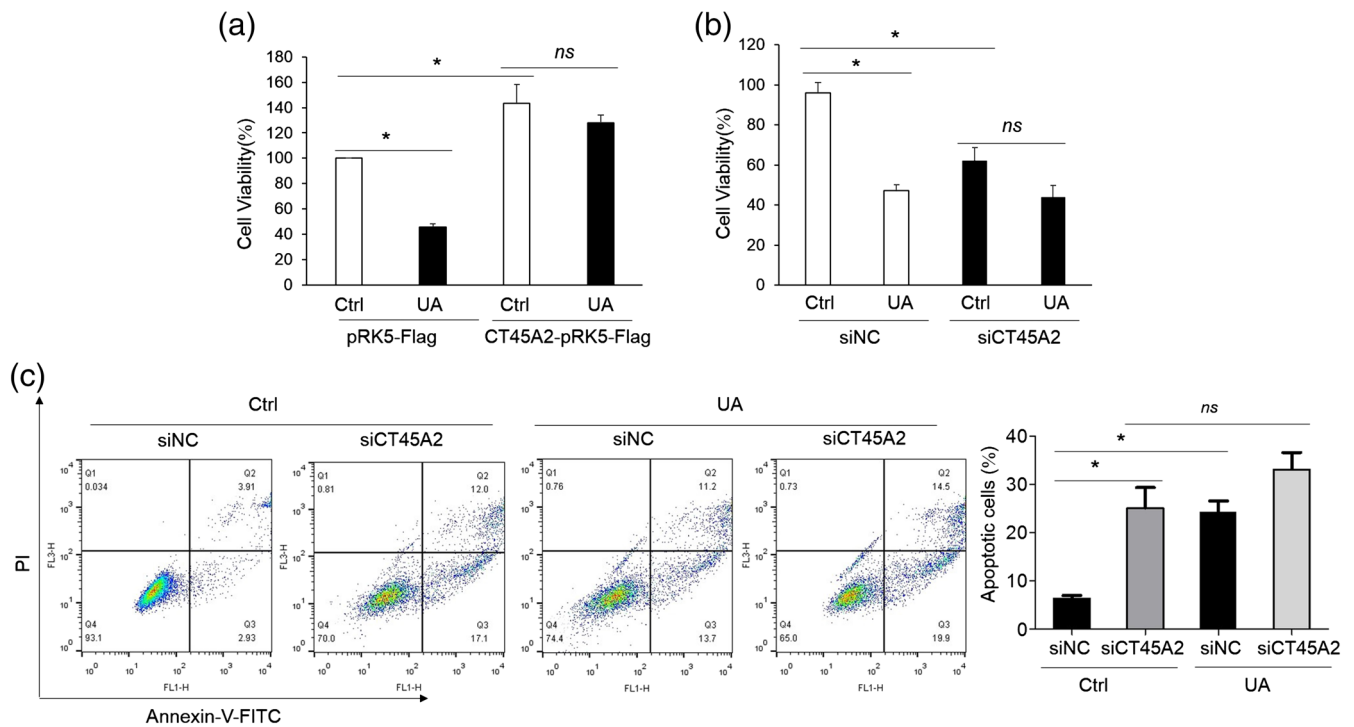


FIGURE 4 Ursolic acid (UA) induced cell apoptosis and inhibited cell motility in H1975 cells harbouring the EGFR L858R/T790M mutation. (A) H1975 cells were transfected with CT45A2-pRK5-Flag or pRK5-Flag and then cells were incubated with UA (25 $\mu\text{mol/L}$) for 24 hr, Cell viability was evaluated using by MTT proliferation assay. (B) H1975 cells were transfected with siRNA against CT45A2 (siCT45A2) or a negative control siRNA (siNC). the indicated gene was detected by PCR. Cell viability was evaluated using by MTT assay. (C) H1975 cells were treated with UA (25 $\mu\text{mol L}^{-1}$) and then stained with AnnexinV-FITC and propidium iodide for detecting apoptosis by flow cytometry. Data shown are means \pm SD from five independent experiments. * $P < 0.05$, significantly different as indicated; ns, non-significant effects

silencing (Figure 6A). We then assessed the dependence on TCF4 of the inhibition of the proliferation of H1975 cells by UA. MTT assay indicated that the suppressive effect of UA on H1975 cells growth was greatly attenuated in TCF4-silenced cells (Figure 6B). In addition, Annexin V-FITC/PI assays also showed that UA-induced apoptosis in H1975 cells was significantly attenuated by TCF4 silencing (Figure 6C), suggesting the effect of UA was dependent on TCF4.

The transcription factor TCF4 is known to be a mediator of Wnt/ β -catenin signalling pathways in development and cancer. Therefore, we investigated the effect of UA on the Wnt/ β -catenin/TCF4 signalling pathway in H1975 cells. As shown in Figure 6d, UA treatment suppressed the phosphorylation of β -catenin at Ser^{33/37}/Thr⁴¹, and the levels of TCF4, along with inducing the phosphorylation of GSK-3 β on Ser⁹ in H1975 cells compared with the control group. However, no significant effect was observed on the protein levels of total β -catenin and GSK-3 β by UA. UA also inhibited the transport of β -catenin into the nucleus which resulted in a marked decrease in β -catenin levels in the nucleus (Figure 6d,e). Thus, the β -catenin/TCF4 signalling pathway was involved in the regulation of TCF4 expression by UA.

Subsequently, we examined whether UA influenced the expression of CT45A2 mRNA in tumours. The expression of CT45A2 mRNA was significantly decreased by treatment with UA (Figure 7a). We then examined the effect of UA on the β -catenin/TCF4 signalling

pathway related to the protein expression in tumour tissues. Western blotting revealed significant reductions in the expression of p- β -catenin (Ser^{33/37}/Thr⁴¹) and TCF4 in tumours from the groups treated with UA, compared with the vehicle group (Figure 7b). Results also indicated that the phosphorylation of GSK3 β (Ser⁹) was increased by UA treatment (Figure 7b). By contrast, erlotinib failed to affect the expression of p- β -catenin, p-GSK3 β , or TCF4. Immunohistochemical analysis of xenograft tumour tissues from vehicle- or UA-treated animals showed that treatment with UA increased the cleavage of caspase-3 in tumour tissue (Figure 7c). In contrast, erlotinib failed to affect caspase-3 cleavage (Figure 7c).

4 | DISCUSSION

In this study, our results showed that CT45A2 up-regulation is associated with a second mutation in the EGFR kinase domain. CT45A2 is a proto-oncogene which plays an important role in promoting tumourigenesis and enhancing cell motility. Our data have also shown that UA inhibited CT45A2 expression and cell proliferation, motility, and promoted apoptosis in NSCLCs harbouring the EGFR T790M mutation. A possible mechanism of this suppression is via the inhibition of the β -catenin/TCF4 pathway which further down-regulates the expression of CT45A2 (Figure 8).

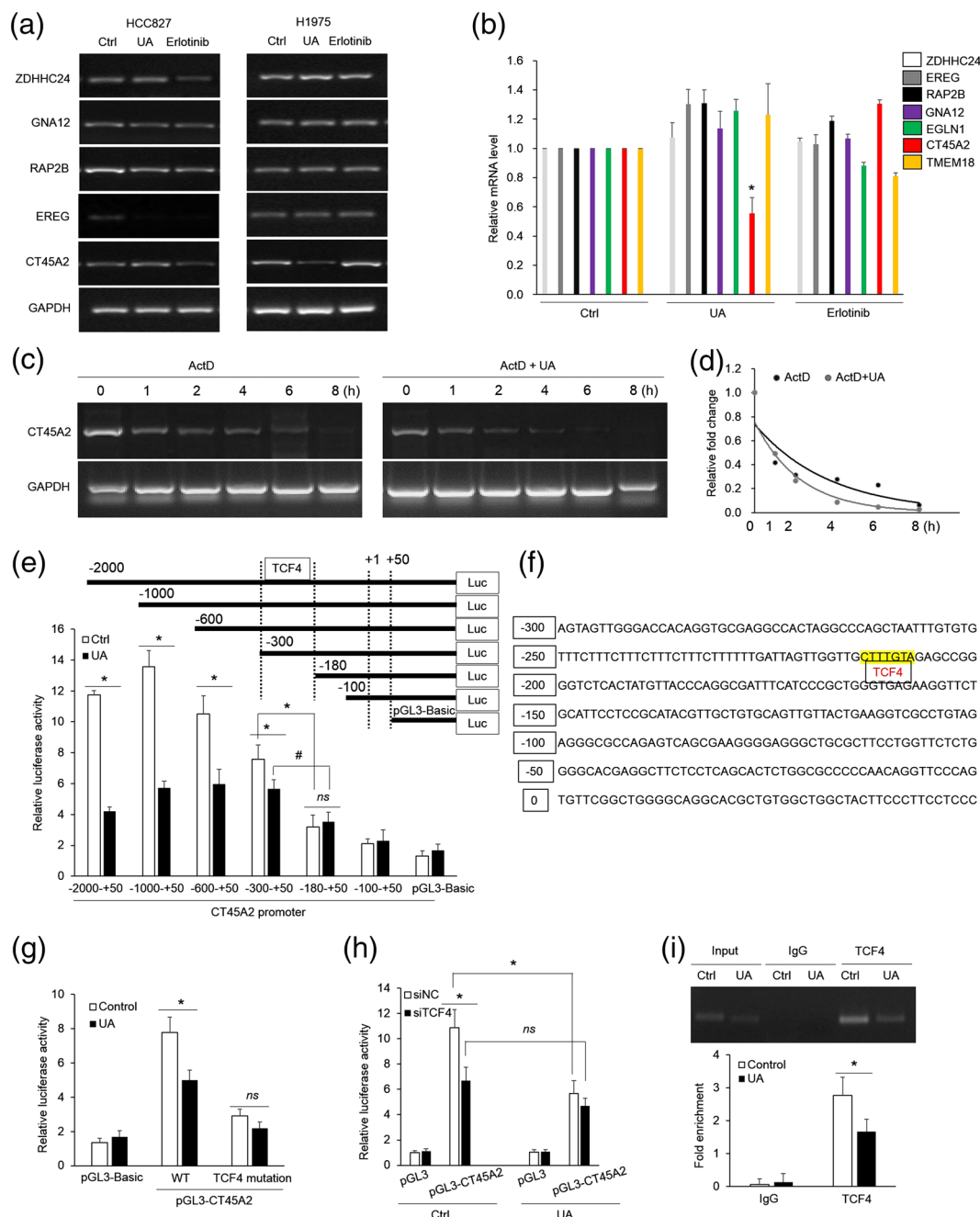


FIGURE 5 Ursolic acid (UA) inhibited the CT45A2 gene promoter through TCF4 sites in H1975 cells. (A) HCC827 and H1975 cells were incubated with UA ($25 \mu\text{mol L}^{-1}$) and erlotinib ($5 \mu\text{mol L}^{-1}$) for 12 hr. The total RNA of above-treated cells was extracted, and RT-PCR was performed to examine the mRNA level of the indicated genes (ZDHHC24, EREG, RAP2B, GNA12, CT45A2). (B) H1975 cells were treated with UA ($25 \mu\text{mol L}^{-1}$) and erlotinib ($5 \mu\text{mol L}^{-1}$) for 12 hr. The total RNA of above-treated cells was extracted, Q-PCR was performed to examine the mRNA levels of indicated genes (ZDHHC24, EREG, RAP2B, GNA12, EGLN1, CT45A2, TMEM18). The endogenous β -actin RNA was used as the internal control. (C) UA ($25 \mu\text{mol L}^{-1}$) did not affect the half-life of mRNA for CT45A2 in H1975 cells. Actinomycin D (Act D, $4 \mu\text{g mL}^{-1}$) was added after 4hr UA treatment of H1975 cells. The cells were harvested for total RNA extraction at the indicated time, and mRNA levels were measured with PCR. GAPDH is used as a control. (D) CT45A2 expression levels assessed by semi-quantitative PCR analysis. (E) Serial deletion mutant analysis of the CT45A2 promoter. H1975 cells were transfected with the human CT45A2 promoter-luciferase construct and were incubated without or with UA ($25 \mu\text{mol L}^{-1}$) for 12 hr. the transcriptional activity of truncated CT45A2s was determined by dual-luciferase reporter assay. (F) The transcription factor binding sites of human CT45A2 gene were predicted by *PROMO HOME PAGE*. (G) The CT45A2 promoter constructs with mutation in specific TCF4 sites were transfected into cells and the luciferase activity was determined to identify the specific TCF4 binding site involved in the regulation of CT45A2 promoter activity by UA. (H) Knockdown of TCF4 decreased CT45A2 luciferase reporter activity in H1975 cells. (I) The binding of TCF4 to CT45A2 promoter were studied by ChIP assay combined with PCR. The β -actin gene was used as an internal control. Data shown are means \pm SD from five independent experiments. * $P < 0.05$, # $P < 0.05$, significantly different as indicated; ns, non-significant effects

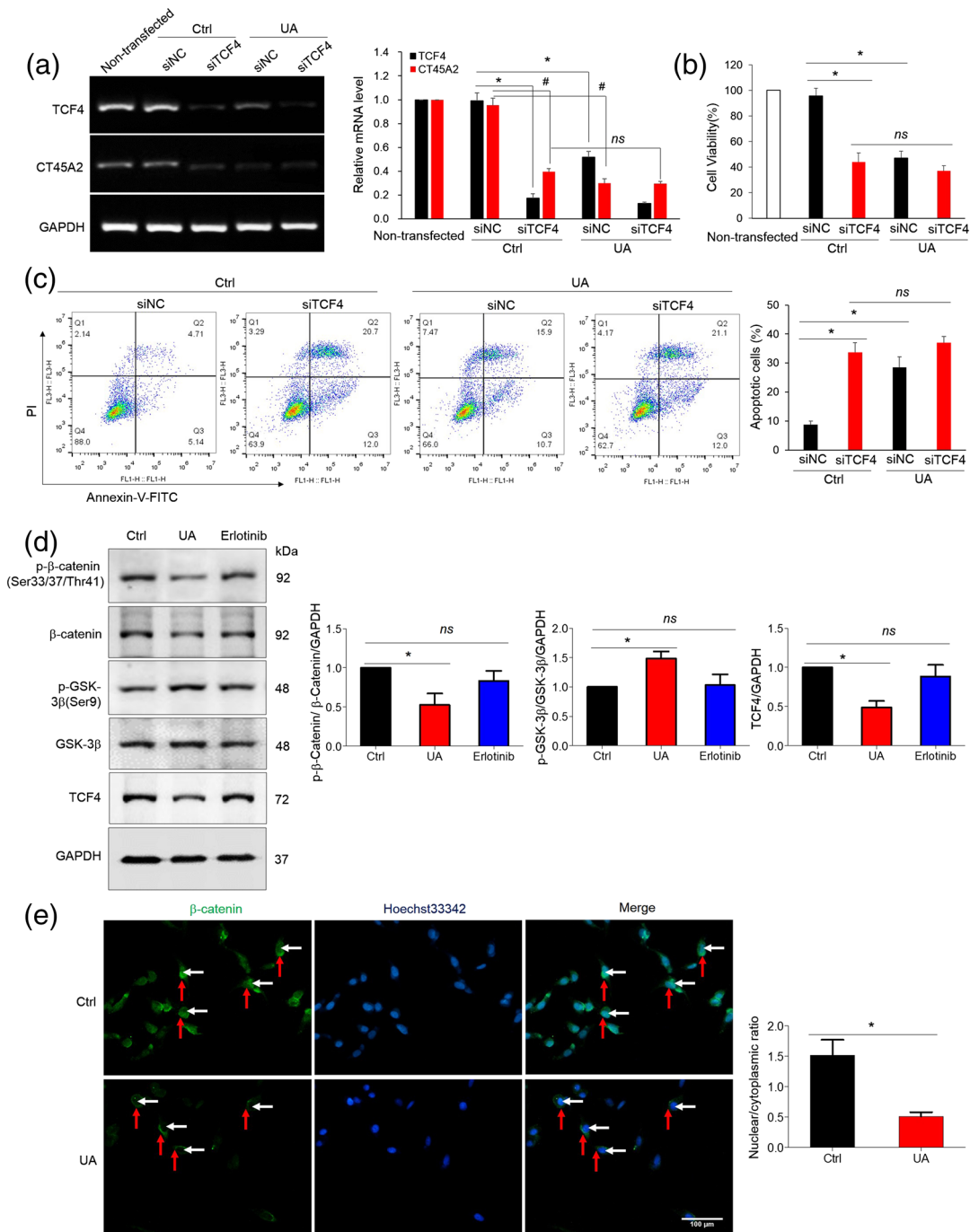


FIGURE 6 Ursolic acid (UA) inhibited β -catenin/TCF4 signalling pathway in H1775 cells. (A) Left: H1775 cells, with or without transfection with siRNA against TCF4 (siTCF4) or a negative control siRNA (siNC), were incubated with PBS or UA ($25 \mu\text{mol L}^{-1}$) for 8 hr. The indicated gene was detected by PCR. Right: TCF4 and CT45A2 mRNA levels in Fig. 6A, as analyzed by Image J software. (B) H1775 cells, with or without transfection with siRNA against TCF4 (siTCF4) or a negative control siRNA (siNC), were incubated with PBS or UA for 24 hr, cell viability was evaluated using by MTT assay. (C) H1775 cells, with or without transfection with siRNA against TCF4 (siTCF4) or a negative control siRNA (siNC), were incubated with PBS or UA for 24 hr, and then stained with AnnexinV-FITC and propidium iodide for detecting apoptosis by flow cytometry. The graph shows the mean values from FACS assays. (D) Left: Protein expression of β -catenin, GSK-3 β and their phosphorylated forms, were determined by western blot analysis. Phosphorylation of β -catenin and GSK-3 β was decreased after UA treatment. Erlotinib was used as the negative control. Right: The graph shows the mean values from western blotting. Protein levels were quantified using gray value analyses by Image J software. (E) Left: UA inhibited β -catenin into the nucleus. H1775 cells were treated with UA stimuli for 24 hr, the distribution of β -catenin (green) was detected by immunofluorescence. The nucleus was visualized by Hoechst33342 staining. White arrows indicate the nucleus. Red arrows indicate the cytoplasm. Scale bar=100 μm . Right: Quantification of β -catenin nuclear/cytoplasmic ratio in Fig.6E. Mean of nuclear/cytoplasmic ratios were calculated from 30 H1775 cells. Mean pixel intensity was calculated using GNU Image Manipulator. Data shown are means \pm SD from five independent experiments * $P < 0.05$, # $P < 0.05$, significantly different as indicated; ns, non-significant effects

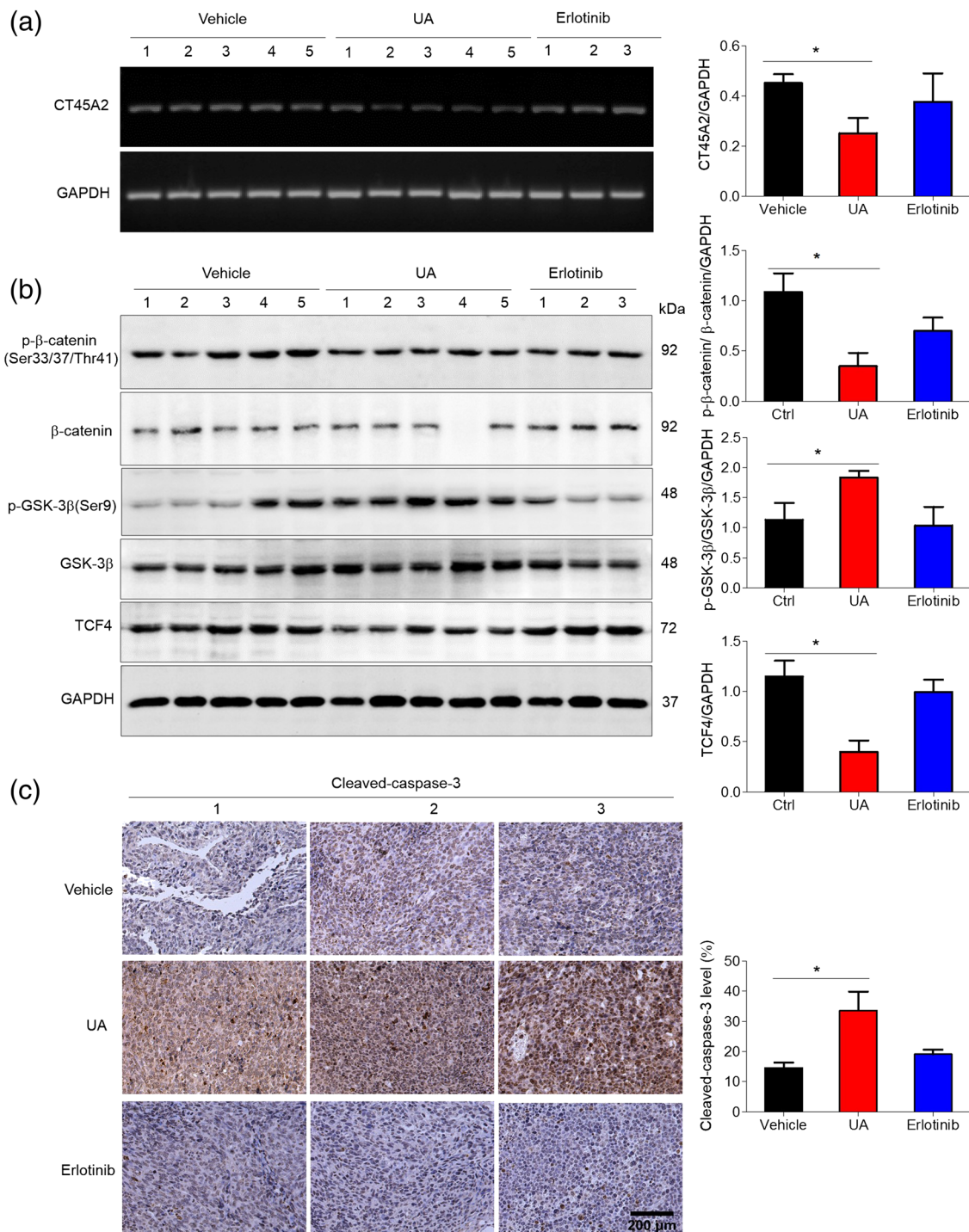


FIGURE 7 Ursolic acid (UA) inhibited CT45A2 mRNA expression and β-catenin/TCF4 signalling pathway in vivo. (A) Left: UA inhibited CT45A2 mRNA expression in tumour tissues. Tumour tissues from groups treated with vehicle, UA (25 mg kg⁻¹) or erlotinib (20 mg kg⁻¹), were harvested for total RNA extraction and mRNA levels were measured with PCR. GAPDH is used as a control. Right: CT45A2 mRNA levels in Fig. 7A, as analyzed by Image J software. (B) Left: UA inhibited β-catenin/TCF4 signalling protein expression in tumour tissues. Tumour tissues from groups treated with vehicle, UA (25 mg kg⁻¹) or erlotinib (20 mg kg⁻¹), were immunoblotted with antibodies to detect β-catenin, GSK-3β, p-β-catenin(Ser^{33/37}/Thr⁴¹), p-GSK-3β(Ser⁹), TCF4 and GAPDH. Right: Analysis of western blotting results in Fig. 7B. Protein levels were quantified using gray value analyses by Image J software. (C) Left: Immunohistochemical analysis of the cleaved-caspase3 expression in xenograft tumours formed by H1975 cells in mice treated with vehicle, UA, or erlotinib. Representative images are shown. Scale bar=200 μm. Right: quantitative analysis of the immunohistochemical staining by using Image J software. Data shown are means ± SD from five independent experiments for vehicle group and UA group; three independent experiments for erlotinib group. *P < 0.05, significantly different as indicated; ns, non-significant effects

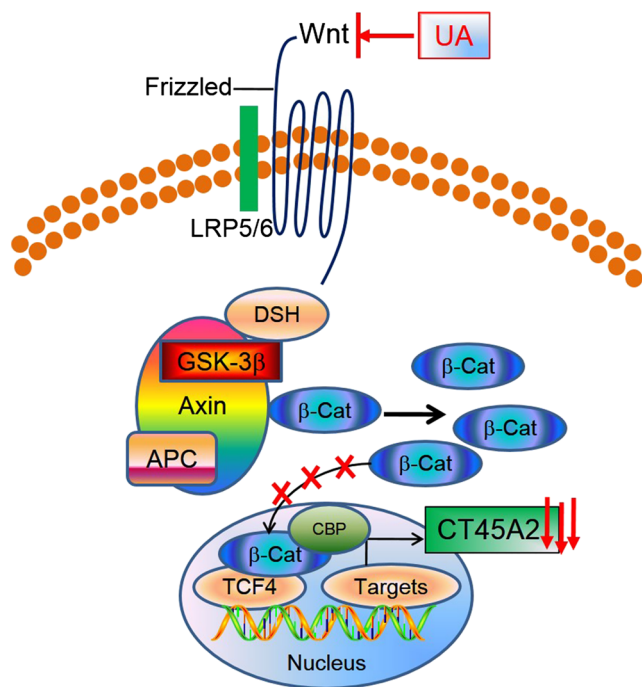


FIGURE 8 Diagram of the mechanism by which ursolic acid (UA) exhibits anti-neoplastic activity on H1975 cells via regulating Wnt signalling and CT45A2 expression. CT45A2 is a novel pro-oncogene in H1975 cells with the EGFR T790M mutation that can promote tumour growth. In addition, CT45A2 is also a target gene of Wnt signalling. UA suppressed TCF4-mediated CT45A2 gene expression, and thereby leading to growth arrest and apoptosis of H1975 cells

CT45A2 belongs to the CTA-45 (CT45) family. CTAs are aberrantly expressed in various cancer types, particularly in advanced cancers, but normally expressed only in the adult testis. The biological function of CTAs is to increase cell stemness, tumourigenesis, invasion, and metastasis and to promote the epithelial–mesenchymal transition (Almeida *et al.*, 2009; Kalejs *et al.*, 2005; Kulkarni *et al.*, 2012; Odunsi *et al.*, 2003; Old, 2001). However, the role of CT45A2 in NSCLC harbouring EGFR T790M mutations has not been reported. Our study provides strong evidence that CT45A2 is specifically up-regulated in H1975 cells harbouring EGFR T790M and plays a protective role in lung cancer. Previous reports state that CT45A1, another CT45 member, promotes the growth and metastasis of breast cancer (Shang *et al.*, 2014). Our data also showed that CT45A2 is associated with a second mutation in the EGFR kinase domain. The over-expression of CT45A2 in H1975 cells markedly promoted proliferation and motility, whereas silencing CT45A2 significantly reduced cancer cell motility and survival. There is good evidence that CT45A2 functions as a novel proto-oncogene to trigger oncogenesis and motility. However, the mechanisms of CT45A2-mediated oncogenesis and cancer cell motility have not been determined. Previous reports indicated that CT45A1 promoted expression of pro-oncogenic genes (MAGED4B, HOXB6, HOXD13, and RASGEF1A) and EMT-related genes (TWIST1, ALDH1A1, and KIT) in breast cancer (Shang *et al.*,

2014). As observed for many other CTAs, CT45A2 may also have related biological functions. Although further study is needed, these data suggest that CT45A2 activation is probably a novel mechanism underlying drug resistance to EGFR-TKIs in, at least, NSCLC cells harbouring the EGFR T790M mutation. Therefore, further study of the oncogenic effects and mechanisms of CT45A2 and other CT45 family members should reveal new insights into tumourigenesis and specific tumour therapy.

Our data have shown that UA can inhibit the expression of CT45A2 mRNA. However, how UA regulates CT45A2 expression was not clear. Hence, the role of UA-induced down-regulation of CT45A2 mRNA in mediating the pro-apoptotic and antiproliferative activities of this compound was further investigated in H1975 cells. We have proposed that UA suppressed CT45A2 gene expression at the level of mRNA transcription (Nair *et al.*, 2013). To confirm whether UA regulated the transcriptional activity of the promoter regions of CT45A2, CT45A2 expressing plasmid luciferase reporters were transfected into H1975 cells. UA significantly decreased the promoter activity of CT45A2. Further analysis found that the transcription factor TCF4 plays a pivotal role in the CT45A2 gene transcription. Mutation or knockdown of TCF4 decreased CT45A2 luciferase activity. Previous studies have demonstrated that TCF4 recognizes CTTTGTA motifs, acting as a transcriptional activator or suppressor. To examine the physical binding of TCF4 with the promoters of CT45A2, ChIP assay was carried out. The results of this experiment demonstrated that TCF4 bound to CTTTGTA motifs of the CT45A2 promoter. Our data also showed that UA decreased TCF4 binding to CTTTGTA in the promoter of CT45A2 and confirmed that UA suppressed the transcription of CT45A2.

The transcription factor TCF4 is regulated by the Wnt/ β -catenin signalling pathway. β -catenin/TCF4 signals are involved in a range of biological processes in various types of human cancers, including lung cancer (Clevers *et al.*, 2012; Kahn, 2014; Rotow *et al.*, 2017). Many cancers acquire drug resistance due to the activation of the Wnt/ β -catenin pathway (Rotow *et al.*, 2017; Yamaguchi *et al.*, 2014). In particular, the anti-tumour activity of UA on osteosarcoma may be mediated by inactivating Wnt/ β -catenin signalling through upregulating p53 (Zhang *et al.*, 2016). Our present results also showed that UA treatment substantially suppressed β -catenin phosphorylation at Ser^{33/37}/Thr⁴¹ and increased GSK-3 β phosphorylation at Ser⁹ in H1975 cells. In agreement with these results, mice bearing lung cancer (H1975 cells) treated with UA showed marked decrease in β -catenin phosphorylation at Ser^{33/37}/Thr⁴¹ and activated GSK-3 β phosphorylation at Ser⁹. We also observed that UA suppressed TCF4 protein expression and nuclear translocation of β -catenin. The cytosolic retention of β -catenin prevents the transactivation of downstream target genes such as TCF4, cyclin D1, c-myc, and Axin2 (Clevers & Nusse, 2012; Clevers, 2006; Zhan, Rindtorff, & Boutros, 2017; Kahn, 2014). These results indicated that UA decreased expression of CT45A2 in H1975 cells. This response mechanism is at least in part mediated by blocking the nuclear translocation of β -catenin protein, thereby inhibiting β -catenin/TCF4 transcriptional activity.

The T790M mutation of the EGFR is present in about half of the lung cancer patients with acquired resistance. Thus, our finding that UA exerted antitumour effects in the xenograft model by inhibiting the β -catenin/TCF4 signalling pathway and its downstream target CT45A2, leading to the inhibition of proliferation and motility, suggests that UA has significant potential for the treatment of NSCLC harbouring the EGFR T790M mutant. As the doses of UA (25 mg·kg⁻¹) used in our animal study are safe and relevant to that in human subjects, the current study provides a basis for evaluating the efficacy of UA in clinical trials. Importantly, based on our study, UA may be considered as a potential therapeutic choice for the treatment of patients with NSCLC harbouring the EGFR T790M mutation.

To sum up, these data have demonstrated that CT45A2 is a novel proto-oncogene for lung cancers expressing EGFRs with the T790M mutation. The data have also shown that UA induced apoptosis and inhibited the proliferation of H1975 cells through negatively regulating the β -catenin/TCF4/CT45A2 signalling pathway.

ACKNOWLEDGEMENTS

This project was sponsored by the National Natural Science Foundation of China (81673462, 81671939, 81473293, 81403347, 81573604, 81774269, 81874452 and 91540119), the Fundamental Research Funds for the Central Universities, Six Talent Peaks Project in Jiangsu Province to Y.W. (YY-012), and Key Development Project of Jiangsu Province (BE2017712).

CONFLICT OF INTEREST

The authors declare no conflicts of interest.

AUTHOR CONTRIBUTIONS

K.Y. designed and carried out all of the experiments, processed the experimental data and performed the analysis, made the figures, and drafted the manuscript. W.Y. X.H., Z.T., and Y.C. came up with the original idea and designed the study, interpreted the results, and supervised the study. L.M., Y.S., X.C., and Y.W. helped to bred the Balb/C nude mice and measure tumour volume. Z.Z., X.J., and L.C. aided in constructing plasmids. J.Z. assisted with haematoxylin-eosin staining experiments and checked the references. H.D., B.Z., and C.L. contributed to sample preparation. All authors provided critical feedback and helped shape the research, analysis, and manuscript.

DECLARATION OF TRANSPARENCY AND SCIENTIFIC RIGOUR

This Declaration acknowledges that this paper adheres to the principles for transparent reporting and scientific rigour of preclinical research as stated in the *BJP* guidelines for [Design & Analysis](#), [Immunoblotting and Immunochemistry](#), and [Animal Experimentation](#), and as recommended by funding agencies, publishers, and other organizations engaged with supporting research.

ORCID

Wu Yin  <https://orcid.org/0000-0001-8859-7865>

REFERENCES

- Alexander, S. P. H., Fabbro, D., Kelly, E., Mathie, A., Peters, J. A., Veale, E. L., ... Collaborators, C. G. T. P. (2019a). The Concise Guide to PHARMACOLOGY 2019/20: Catalytic receptors. *British Journal of Pharmacology*, 176, S247–S296. <https://doi.org/10.1111/bph.14751>
- Alexander, S. P. H., Fabbro, D., Kelly, E., Mathie, A., Peters, J. A., Veale, E. L., ... Collaborators, C. G. T. P. (2019b). The Concise Guide to PHARMACOLOGY 2019/20: Enzymes. *British Journal of Pharmacology*, 176, S297–S396. <https://doi.org/10.1111/bph.14752>
- Alexander, S. P. H., Kelly, E., Mathie, A., Peters, J. A., Veale, E. L., Faccenda, E., ... Collaborators, C. G. T. P. (2019). The Concise Guide to PHARMACOLOGY 2019/20: Introduction and Other Protein Targets. *British Journal of Pharmacology*, 176, S1–S20. <https://doi.org/10.1111/bph.14747>
- Almeida, L. G., Sakabe, N. J., deOliveira, A. R., Silva, M. C., Mundstein, A. S., Cohen, T., ... Vasconcelos, A. T. (2009). CTdatabase: A knowledge-base of high-throughput and curated data on cancer-testis antigens. *Nucleic Acids Research*, 37, D816–D819. <https://doi.org/10.1093/nar/gkn673>
- Chong, C. R., & Janne, P. A. (2013). The quest to overcome resistance to EGFR-targeted therapies in cancer. *Nature Medicine*, 19, 1389–1400. <https://doi.org/10.1038/nm.3388>
- Clevers, H. (2006). Wnt/ β -catenin signaling in development and disease. *Cell*, 127, 469–480. <https://doi.org/10.1016/j.cell.2006.10.018>
- Clevers, H., & Nusse, R. (2012). Wnt/ β -catenin signaling and disease. *Cell*, 149, 1192–1205. <https://doi.org/10.1016/j.cell.2012.05.012>
- Cross, D. A., Ashton, S. E., Ghiorghiu, S., Eberlein, C., Nebhan, C. A., Spitzler, P. J., ... Pao, W. (2014). AZD9291, an irreversible EGFR TKI, overcomes T790M-mediated resistance to EGFR inhibitors in lung cancer. *Cancer Discovery*, 4, 1046–1061. <https://doi.org/10.1158/2159-8290.CD-14-0337>
- Curtis, M. J., Alexander, S., Cirino, G., Docherty, J. R., George, C. H., Giermycz, M. A., et al. (2018). Experimental design and analysis and their reporting II: updated and simplified guidance for authors and peer reviewers. *Br J Pharmacol*, 175, 987–993.
- Gao, S. P., Mark, K. G., Leslie, K., Pao, W., Motoi, N., Gerald, W. L., ... Bromberg, J. F. (2007). Mutations in the EGFR kinase domain mediate STAT3 activation via IL-6 production in human lung adenocarcinomas. *The Journal of Clinical Investigation*, 117, 3846–3856. <https://doi.org/10.1172/JCI31871>
- Harding, S. D., Sharman, J. L., Faccenda, E., Southan, C., Pawson, A. J., Ireland, S., ... NC-IUPHAR (2018). The IUPHAR/BPS Guide to PHARMACOLOGY in 2018: Updates and expansion to encompass the new guide to IMMUNOPHARMACOLOGY. *Nucleic Acids Research*, 46, D1091–D1106.
- Hata, A. N., Niederst, M. J., Archibald, H. L., Gomez-Caraballo, M., Siddiqui, F. M., Mulvey, H. E., ... Engelman, J. A. (2016). Tumor cells can follow distinct evolutionary paths to become resistant to epidermal growth factor receptor inhibition. *Nature Medicine*, 22, 262–269. <https://doi.org/10.1038/nm.4040>
- Kashyap, D., Tuli, H. S., & Sharma, A. K. (2016). Ursolic acid (UA): A metabolite with promising therapeutic potential. *Life Sciences*, 146, 201–213. <https://doi.org/10.1016/j.lfs.2016.01.017>
- Kilkenny, C., Browne, W., Cuthill, I. C., Emerson, M., & Altman, D. G. (2010). Animal research: Reporting in vivo experiments: The ARRIVE guidelines. *British Journal of Pharmacology*, 160, 1577–1579.
- Kim, J. H., Kim, Y. H., Song, G. Y., Kim, D. E., Jeong, Y. J., Liu, K. H., ... Oh, S. (2014). Ursolic acid and its natural derivative corosolic acid suppress the proliferation of APC-mutated colon cancer cells through promotion of β -catenin degradation. *Food and Chemical Toxicology*, 67, 87–95. <https://doi.org/10.1016/j.fct.2014.02.019>
- Kim, S. H., Ryu, H. G., Lee, J., Shin, J., Harikishore, A., Jung, H. Y., ... Kim, K. T. (2015). Ursolic acid exerts anti-cancer activity by suppressing vaccinia-related kinase 1-mediated damage repair in lung cancer cells. *Scientific Reports*, 5, 14570. <https://doi.org/10.1038/srep14570>

- Kim, S. M., Kwon, O. J., Hong, Y. K., Kim, J. H., Solca, F., Ha, S. J., ... Cho, B. C. (2012). Activation of IL-6R/JAK1/STAT3 signaling induces de novo resistance to irreversible EGFR inhibitors in non-small cell lung cancer with T790M resistance mutation. *Molecular Cancer Therapeutics*, *11*, 2254–2264. <https://doi.org/10.1158/1535-7163.MCT-12-0311>
- Kim, Y., Ko, J., Cui, Z., Abolhoda, A., Ahn, J. S., Ou, S. H., ... Park, K. (2012). The EGFR T790M mutation in acquired resistance to an irreversible second-generation EGFR inhibitor. *Molecular Cancer Therapeutics*, *11*, 784–791. <https://doi.org/10.1158/1535-7163.MCT-11-0750>
- Kulkarni, P., Shiraishi, T., Rajagopalan, K., Kim, R., Mooney, S. M., & Getzenberg, R. H. (2012). Cancer/testis antigens and urological malignancies. *Nature Reviews. Urology*, *9*, 386–396. <https://doi.org/10.1038/nrurol.2012.117>
- Laszczyk, M. N. (2009). Pentacyclic triterpenes of the lupane, oleanane and ursane group as tools in cancer therapy. *Planta Medica*, *75*, 1549–1560. <https://doi.org/10.1055/s-0029-1186102>
- Nair, V., Pathi, S., Jutooru, I., Sreevalsan, S., Basha, R., Abdelrahim, M., ... Safe, S. (2013). Metformin inhibits pancreatic cancer cell and tumor growth and downregulates Sp transcription factors. *Carcinogenesis*, *34*, 2870–2879. <https://doi.org/10.1093/carcin/bgt231>
- Odunsi, K., Jungbluth, A. A., Stockert, E., Qian, F., Gnjjatic, S., Tammela, J., ... Old, L. J. (2003). NY-ESO-1 and LAGE-1 cancer-testis antigens are potential targets for immunotherapy in epithelial ovarian cancer. *Cancer Research*, *63*, 6076–6083.
- Old, L. J. (2001). Cancer/testis (CT) antigens—A new link between gametogenesis and cancer. *Cancer Immunity*, *1*, 1.
- Oxnard, G. R., Arcila, M. E., Chmielecki, J., Ladanyi, M., Miller, V. A., & Pao, W. (2011). New strategies in overcoming acquired resistance to epidermal growth factor receptor tyrosine kinase inhibitors in lung cancer. *Clinical Cancer Research*, *17*, 5530–5537. <https://doi.org/10.1158/1078-0432.CCR-10-2571>
- Pao, W., Miller, V. A., Politi, K. A., Riely, G. J., Somwar, R., Zakowski, M. F., ... Varmus, H. (2005). Acquired resistance of lung adenocarcinomas to gefitinib or erlotinib is associated with a second mutation in the EGFR kinase domain. *PLoS Medicine*, *2*, e73. <https://doi.org/10.1371/journal.pmed.0020073>
- Rotow, J., & Bivona, T. G. (2017). Understanding and targeting resistance mechanisms in NSCLC. *Nature Reviews. Cancer*, *17*, 637–658. <https://doi.org/10.1038/nrc.2017.84>
- Salvador, J. A. R., Leal, A. S., Valdeira, A. S., Goncalves, B. M. F., Alho, D. P. S., Figueiredo, S. A. C., ... Mendes, V. I. S. (2017). Oleanane-, ursane-, and quinone methide friedelane-type triterpenoid derivatives: Recent advances in cancer treatment. *European Journal of Medicinal Chemistry*, *142*, 95–130. <https://doi.org/10.1016/j.ejmech.2017.07.013>
- Shang, B., Gao, A., Pan, Y., Zhang, G., Tu, J., Zhou, Y., ... Zhou, Q. (2014). CT45A1 acts as a new proto-oncogene to trigger tumorigenesis and cancer metastasis. *Cell Death & Disease*, *5*, e1285. <https://doi.org/10.1038/cddis.2014.244>
- Shanmugam, M. K., Dai, X., Kumar, A. P., Tan, B. K., Sethi, G., & Bishayee, A. (2013). Ursolic acid in cancer prevention and treatment: Molecular targets, pharmacokinetics and clinical studies. *Biochemical Pharmacology*, *85*, 1579–1587. <https://doi.org/10.1016/j.bcp.2013.03.006>
- Shanmugam, M. K., Rajendran, P., Li, F., Nema, T., Vali, S., Abbasi, T., ... Sethi, G. (2011). Ursolic acid inhibits multiple cell survival pathways leading to suppression of growth of prostate cancer xenograft in nude mice. *Journal of Molecular Medicine (Berlin, Germany)*, *89*, 713–727. <https://doi.org/10.1007/s00109-011-0746-2>
- Stewart, E. L., Tan, S. Z., Liu, G., & Tsao, M. S. (2015). Known and putative mechanisms of resistance to EGFR targeted therapies in NSCLC patients with EGFR mutations—a review. *Transl Lung Cancer Res*, *4*, 67–81. <https://doi.org/10.3978/j.issn.2218-6751.2014.11.06>
- Terai, H., Soejima, K., Yasuda, H., Nakayama, S., Hamamoto, J., Arai, D., ... Betsuyaku, T. (2013). Activation of the FGF2-FGFR1 autocrine pathway: A novel mechanism of acquired resistance to gefitinib in NSCLC. *Molecular Cancer Research*, *11*, 759–767. <https://doi.org/10.1158/1541-7786.MCR-12-0652>
- Thress, K. S., Paweletz, C. P., Felip, E., Cho, B. C., Stetson, D., Dougherty, B., ... Oxnard, G. R. (2015). Acquired EGFR C797S mutation mediates resistance to AZD9291 in non-small cell lung cancer harboring EGFR T790M. *Nature Medicine*, *21*, 560–562. <https://doi.org/10.1038/nm.3854>
- Vo, N. N. Q., Fukushima, E. O., & Muranaka, T. (2017). Structure and hemolytic activity relationships of triterpenoid saponins and saponinins. *Journal of Natural Medicines*, *71*, 50–58. <https://doi.org/10.1007/s11418-016-1026-9>
- Walter, A. O., Sjin, R. T., Haringsma, H. J., Ohashi, K., Sun, J., Lee, K., ... Allen, A. (2013). Discovery of a mutant-selective covalent inhibitor of EGFR that overcomes T790M-mediated resistance in NSCLC. *Cancer Discovery*, *3*, 1404–1415. <https://doi.org/10.1158/2159-8290.CD-13-0314>
- Wang, S., Cang, S., & Liu, D. (2016). Third-generation inhibitors targeting EGFR T790M mutation in advanced non-small cell lung cancer. *Journal of Hematology & Oncology*, *9*, 34. <https://doi.org/10.1186/s13045-016-0268-z>
- Wangari-Talbot, J., & Hopper-Borge, E. (2013). Drug resistance mechanisms in non-small cell lung carcinoma. *J Can Res Updates*, *2*, 265–282. <https://doi.org/10.6000/1929-2279.2013.02.04.5>
- Xiang, L., Chi, T., Tang, Q., Yang, X., Ou, M., Chen, X., ... Jia, L. (2015). A pentacyclic triterpene natural product, ursolic acid and its prodrug US597 inhibit targets within cell adhesion pathway and prevent cancer metastasis. *Oncotarget*, *6*, 9295–9312.
- Yamaguchi, H., Chang, S. S., Hsu, J. L., & Hung, M. C. (2014). Signaling cross-talk in the resistance to HER family receptor targeted therapy. *Oncogene*, *33*, 1073–1081. <https://doi.org/10.1038/onc.2013.74>
- Zhan, T., Rindtorff, N., & Boutros, M. (2017). Wnt signaling in cancer. *Oncogene*, *36*, 1461–1473. <https://doi.org/10.1038/ncr.2016.304>
- Zhang, R. X., Li, Y., Tian, D. D., Liu, Y., Nian, W., Zou, X., ... He, B. C. (2016). Ursolic acid inhibits proliferation and induces apoptosis by inactivating Wnt/β-catenin signaling in human osteosarcoma cells. *International Journal of Oncology*, *49*, 1973–1982. <https://doi.org/10.3892/ijo.2016.3701>
- Zhang, Z., Lee, J. C., Lin, L., Olivas, V., Au, V., LaFramboise, T., ... Bivona, T. G. (2012). Activation of the AXL kinase causes resistance to EGFR-targeted therapy in lung cancer. *Nature Genetics*, *44*, 852–860. <https://doi.org/10.1038/ng.2330>

SUPPORTING INFORMATION

Additional supporting information may be found online in the Supporting Information section at the end of this article.

How to cite this article: Yang K, Chen Y, Zhou J, et al. Ursolic acid promotes apoptosis and mediates transcriptional suppression of CT45A2 gene expression in non-small-cell lung carcinoma harbouring EGFR T790M mutations. *Br J Pharmacol*. 2019;176:4609–4624. <https://doi.org/10.1111/bph.14793>